JACS
JOURNAL OF THE AMERICAN CHEMICAL SOCIETY

Communication

pubs.acs.org/JACS

Efficient Charge Storage in Dual-Redox Electrochemical Capacitors through Reversible Counterion-Induced Solid Complexation

Brian Evanko,[†,#] Seung Joon Yoo,[*,‡,#] Sang-Eun Chun,[⊥] Xingfeng Wang,[∥] Xiulei Ji,[∥] Shannon W. Boettcher,[*,§] and Galen D. Stucky[*,†,‡]

[†]Materials Department, University of California, Santa Barbara, California 93106, United States
[‡]Department of Chemistry & Biochemistry, University of California, Santa Barbara, California 93106, United States
[⊥]School of Materials Science and Engineering, Kyungpook National University, Daegu 41566, Republic of Korea
[∥]Department of Chemistry, Oregon State University, Corvallis, Oregon 97331, United States
[§]Department of Chemistry & Biochemistry, University of Oregon, Eugene, Oregon 97403, United States

Supporting Information

ABSTRACT: The performance of redox-enhanced electrochemical capacitors (redox ECs) is substantially improved when oxidized catholyte (bromide) and reduced anolyte (viologen) are retained within the porous electrodes through reversible counterion-induced solid complexation. Investigation of the mechanism illustrates design principles and identifies pentyl viologen/bromide (PV/Br) as a new high-performance electrolyte. The symmetric PV/Br redox EC produces a specific energy of 48.5 W·h/kg_{dry} at 0.5 A/g_{dry} (0.44 kW/kg_{dry}) with 99.7% Coulombic efficiency, maintains stability over 10 000 cycles, and functions identically when operated with reversed polarity.

Commercial electric double-layer capacitors (EDLCs) provide specific power as high as 20 kW/kg for millions of cycles, but have a low energy density, compared to other energy storage systems, of ∼6 W·h/kg (8 W·h/L).[1,2] To increase the energy density of EDLCs, research has focused on developing pseudocapacitive systems that add faradaic energy storage.[3−10] One recent approach is to replace the traditional solid-state pseudocapacitive materials with soluble redox couples.[11−16] Such redox-enhanced electrochemical capacitors (redox ECs) provide high power density and increased specific energy without the need for nanostructured metal oxide/nitride electrodes and allow for good performance in aqueous electrolytes. However, they are challenged by poor cycle lifetime and fast internal self-discharge due to cross-diffusion of redox-active electrolytes.[17,18] For efficient redox ECs, the redox couples used should exhibit fast and reversible electron transfer and be retained inside the porous electrodes in their charged states (i.e., oxidized catholyte or reduced anolyte) to eliminate self-discharge.[19]

We recently identified heptyl viologen/bromide (HV/Br) as a promising dual-redox-active electrolyte for aqueous redox ECs (Figure 1a, R = *n*-heptyl).[20] The system maintains cycling stability over 20 000 cycles and has a slow self-discharge rate without using a costly ion-selective membrane as a separator. However, due to the low solubility of HV (<0.2 M), the specific energy was limited to ∼30 W·h/kg_{dry}, i.e., normalized to the dry mass of both the positive electrode (cathode) and negative electrode (anode). Substituting HV with highly soluble methyl viologen (MV) increased the specific energy to 50 W·h/kg_{dry}, but the energy density faded (Figure 1b) and the self-discharge rate increased.[12] One critical challenge is to attain high energy density, stable cycling, and minimal self-discharge in a single device.

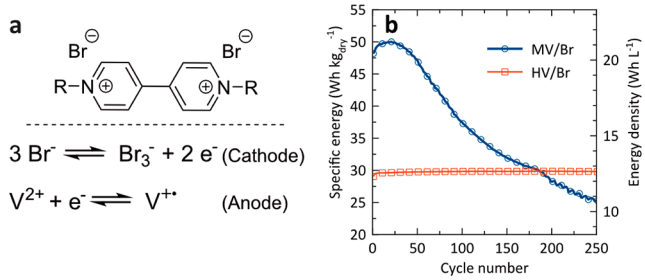

Figure 1. Viologen/bromide redox ECs. (a) Viologen dibromide and faradaic energy storage reactions of bromide and viologen (denoted as V). (b) Cycling stability of redox ECs. Cells are charged to 1.4 V (0.5 M $MVCl_2$/1 M KBr) and 1.2 V (0.1 M $HVBr_2$/0.4 M KBr) at 0.5 A/g_{dry} in custom Swagelok cells (Figure S1).

For the work described in this Communication, we investigated V/Br dual-redox ECs to elucidate the mechanisms underlying the observed cycling behavior. We find that the stability of the HV/Br system is due to the effective retention of charged redox products through reversible electrodeposition/precipitation at the surface of both electrodes. Based on fundamental understanding of the electrolyte chemistry, we rationally design an electrolyte system that incorporates pentyl viologen (PV) as anolyte and bromide as catholyte. This system combines the cycling stability of HV with the solubility of MV to produce a high specific energy of 48.5 W·h/kg_{dry} (20 W·h/L) at 0.5 A/g_{dry} (average specific discharge power of 0.44 kW/kg_{dry}) and maintains stability, with 97% energy retention over 10 000 cycles at 2.5 A/g_{dry} (2.0 kW/kg_{dry}). In addition, we show that the redox EC allows completely symmetric operation

Received: May 17, 2016
Published: July 21, 2016

DOI: 10.1021/jacs.6b05038
J. Am. Chem. Soc. 2016, 138, 9373−9376

without failure or instability when operated with reversed polarity.

In aqueous electrolytes, the 1,1′-substituents of the viologens (1,1′-disubstituted-4,4′-bipyridinium dications) significantly affect the solubility of the cation radical.[21] With bromide as the counterion, viologen dications with alkyl substituents R ≥ 5 (*n*-pentyl) precipitate as the $[V^{+\bullet}\cdot Br^-]$ salt at the electrode surface when reduced.[22,23] Solubility tests of $HV^{+\bullet}$ and $MV^{+\bullet}$ in the presence of KBr indeed show that HV precipitates as the $[HV^{+\bullet}\cdot Br^-]$ salt and $[MV^{+\bullet}\cdot Br^-]$ remains dissolved in solution (Figure S2).

We first investigated whether the difference in solubility of the $[V^{+\bullet}\cdot Br^-]$ salt at the anode affects the overall cycling stability of the cell (Figure 1), noting that the *soluble* $MV^{+\bullet}$ could be susceptible to irreversible reactions (e.g., polymerization).[20] To study the degradation mechanism, we built two asymmetric EC cells, one with the $MV^{2+}/MV^{+\bullet}$ redox couple (0.1 M $MVCl_2$) and the other with the Br^-/Br_3^- redox couple (1 M KBr) for comparison, without any other electrolyte. Counter electrodes were ruled out as a source of fading by oversizing them so that charge storage was only via double-layer capacitance. Galvanostatic charge/discharge (GCD) cycling potential profiles are shown in Figure 2.

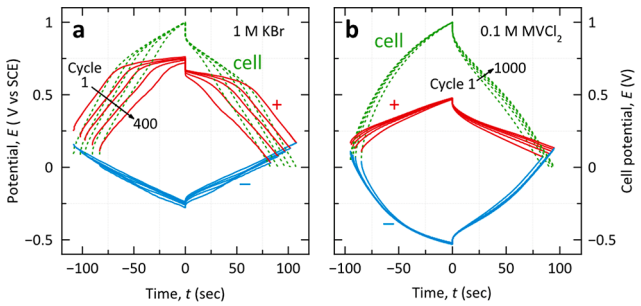

Figure 2. Asymmetric cells. GCD potential profiles for the cathode (+, red curves), anode (−, blue curves), and total cell (green curves) for (a) the first 400 cycles of Br^- catholyte with an EDLC anode (6:1 anode to cathode mass ratio) and (b) the first 1000 cycles of MV^{2+} anolyte with an EDLC cathode (3:1 cathode to anode mass ratio).

The KBr cell degrades rapidly, and over the course of 400 cycles nearly all faradaic charging at the cathode disappears (Figure 2a, red curve). The $MVCl_2$ cell, however, maintains consistent GCD potential profiles for both cathode and anode and even exhibits slight performance improvement over 1000 cycles (Figure 2b, green curve). The stability of the asymmetric $MVCl_2$ cell suggests that although soluble $MV^{+\bullet}$ leads to low Coulombic efficiency and high self-discharge, the $MV^{2+}/MV^{+\bullet}$ redox couple is stable and does not contribute to cell fading. Extended cyclic voltammetry scans of $MVCl_2$/KBr electrolyte at cathodic potentials confirm the reversible redox behavior of MV^{2+} anolyte (Figure S4). With the evidence suggesting that degradation likely occurs at the cathode, we next focused on understanding why the Br^-/Br_3^- redox reaction causes instability when operating alone or in the presence of MV, but remains stable when paired with HV.

Bromide is an efficient catholyte in electrochemical energy storage systems,[24] particularly in aqueous redox flow batteries.[25] However, bromine is corrosive and volatile, and intercalates graphitic carbons.[26] To address these issues, quaternary ammonium salts are used in flow batteries to complex Br_2/Br_3^-, reducing the reactivity and vapor pressure.[27,28] Because viologens are structurally similar to these quaternary ammonium salts, they may also complex Br_2/Br_3^- in redox ECs. We hypothesize that (1) V^{2+} complexes Br_3^- at the cathode, (2) the length of the alkyl substituent determines the solubility of the complex, and (3) HV effectively complexes Br_3^- into an insoluble salt, suppressing its reactivity and cross-diffusion.

To determine if HV is better at precipitating Br_3^- as a solid complex than MV, 20 mM aqueous MV^{2+} or HV^{2+} was measured by ultraviolet−visible (UV−vis) spectroscopy with and without 40 mM Br_3^-. After mixing, 4.0 mM MV^{2+} remained dissolved in solution, as compared to 0.6 mM HV^{2+}. The MV solution also retains a yellow tint from dissolved Br_3^-, while the HV solution turns clear (Figure S3). Greater precipitation of the nominally $[HV^{2+}\cdot 2Br_3^-]$ complex compared to the MV complex is likely driven by the increased hydrophobicity of HV imparted by its longer alkyl substituents.[29] The formation of solid $[HV^{2+}\cdot 2Br_3^-]$ at the cathode should thus suppress the reactivity and diffusion of Br_3^-, allowing the HV/Br cell to cycle stably while the MV/Br cell fades due to the presence of free Br_3^-.

To confirm the role of viologen in complexing Br_3^- and stabilizing the redox ECs, we constructed a cell with higher concentrations of the MV/Br electrolyte (i.e., increasing from 0.5 M $MVCl_2$/1 M KBr to 1 M $MVCl_2$/4 M NaBr). The cell GCD cutoff potential for the concentrated cell was reduced from 1.4 to 1.3 V. Both cells therefore store nearly equal energy, but the concentrated cell has excess Br^- present at the cathode after charging, which facilitates the formation of Br_3^-, and an increased concentration of MV^{2+}, which supports efficient complexation and precipitation of Br_3^-. Over 450 cycles, stability significantly improved from a 62% capacity loss in the original cell to only 17% in the concentrated cell (Figure S7). This result supports the proposed operating mechanism by confirming that cell degradation slows when Br_3^- is more efficiently complexed.

Previously, the slow self-discharge of the halides could not be explained purely by electrostatics and was attributed to the physical adsorption of Br_3^- at the electrode surface suppressing cross-diffusion in the charged state.[13,20] We now show that retention of Br_3^- is driven by the formation of the $[HV^{2+}\cdot 2Br_3^-]$ solid complex at the cathode. Together with the simultaneous generation of the $[HV^{+\bullet}\cdot Br^-]$ solid complex at the anode,[23] the charged products ($HV^{+\bullet}$ and Br_3^-) are immobilized within the porous hydrophobic electrodes, suppressing cross-diffusion (Scheme 1). Microscopic electrodeposition/precipitation occurring at *both* electrodes is consistent with the exceptionally low self-discharge (energy retained after 6 h at open circuit, η_R(6 h) = 86%) and high Coulombic efficiency (99.9%) of the HV/Br device. Therefore, in order to improve the specific energy of V/Br redox ECs

Scheme 1. Charge/Discharge Mechanism of the HV/Br System with Dual Reversible Solid Complexation: Each Ion Acts as a Charge-Storing Redox Couple at One Electrode and as a Complexing Agent at the Other

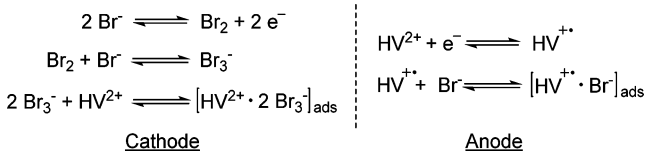

DOI: 10.1021/jacs.6b05038
J. Am. Chem. Soc. 2016, 138, 9373−9376

without compromising on self-discharge or stability, electrolyte design must account for and optimize the dual complexation/precipitation effect.

For redox ECs, high redox-active electrolyte concentrations are advantageous to maximize faradaic energy storage while minimizing electrolyte volume. New viologens to replace MV or HV must (1) be easy to synthesize, (2) have high solubility (≥1 M, *for energy density*), (3) precipitate as a solid complex when reduced at the anode (*for high Coulombic efficiency and slow self-discharge*), and (4) form an insoluble complex with Br_3^- at the cathode (*for stability, Coulombic efficiency, and self-discharge*). Meeting these criteria is challenging because the long hydrophobic alkyl chains that enhance (3) and (4) work against (2) in aqueous systems.

We synthesized a series of alkyl-substituted viologens with R ≥ 5, as viologens with shorter alkyl chains do not precipitate with Br^- upon reduction (Scheme 2 and Table 1).[21] Hexyl

Scheme 2. Synthesis Scheme for Alkyl Viologens

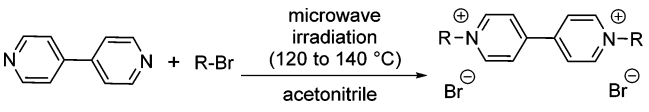

Table 1. Half-Wave Reduction Potential and Solubility for Synthesized Viologens

	no. of CH_2 units	$E_{1/2}$ (V vs SCE)	solubility (M) in 2 M NaBr solution
n-butyl[a]	4	−0.60	>1.5
n-pentyl	5	−0.54	>1.5
n-hexyl	6	−0.50	<0.5
n-heptyl	7	−0.44	<0.2

[a]Butyl viologen is synthesized as well for comparison.

viologen exhibits insufficient solubility (<0.5 M) in the presence of NaBr, but butyl viologen (BV) and pentyl viologen (PV) are highly soluble (>1.5 M). BV and PV were tested for solid complexation with Br_3^- by UV−vis spectroscopy and compared to MV and HV (Figure 3b; see Supporting Information for details). The addition of Br_3^- decreased the concentration of both PV and HV dissolved in the solution by ∼97%, indicating that PV forms a solid complex as effectively as HV. BV shows complexing capacity similar to that of MV.

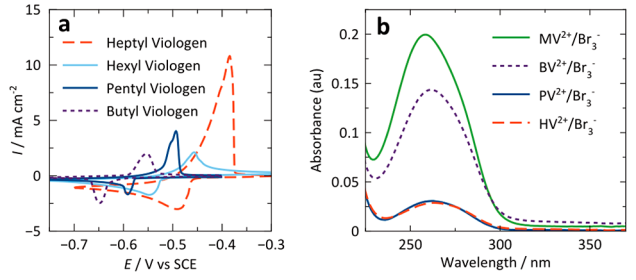

Figure 3. Screening synthesized viologens. (a) Cyclic voltammograms were recorded at a scan rate of 5 mV/s with 20 mM viologen in 0.5 M KBr electrolyte. (b) UV−vis absorption spectra quantifying V^{2+} remaining dissolved in the supernatant after 20 mM V^{2+} complexes and precipitates with 40 mM Br_3^-. Spectra are normalized to absorption maxima of 20 mM V^{2+} solutions without Br_3^- (Figure S5); thus, absorbance peak values here translate to the fraction of the initial V^{2+} that remains uncomplexed.

We selected PV, with both high solubility and good complexing capacity, for further study in dual-redox ECs. A three-electrode cell (Figure 4a) and a two-electrode cell (Figure

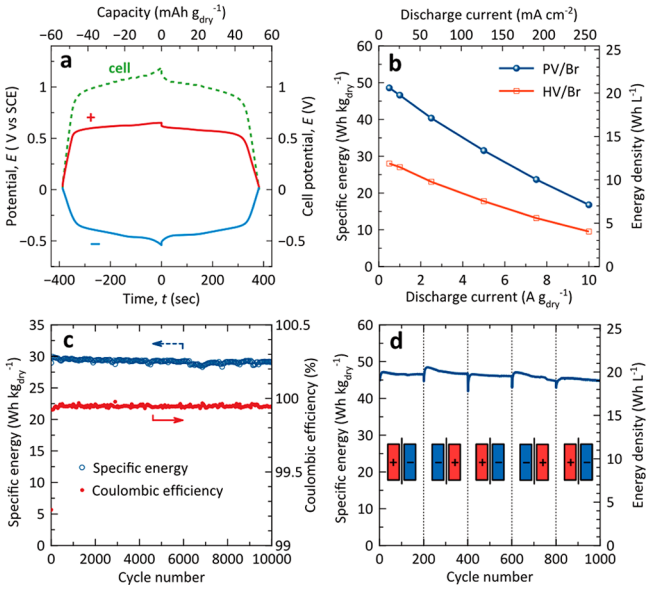

Figure 4. 1 M PVBr2/3 M NaBr cells. (a) GCD potential profiles for the cathode (+, red), anode (−, blue), and total three-electrode cell (green) cycled at 0.5 A/g_{dry}. During charging, the electrochemical behavior transitions from capacitive to faradaic. (b) Specific energy of PV/Br and HV/Br two-electrode cells at different discharge rates. Both cells were charged to 1.2 V at 0.5 A/g_{dry} and discharged at rates from 0.5 to 10 A/g_{dry}. (c) Cycling stability and Coulombic efficiency of PV/Br cell cycled at 2.5 A/g_{dry}. Energy retention is 97% over 10 000 cycles with 99.9% Coulombic efficiency. After 10 000 cycles, the cell achieves the same specific energy at 0.5 A/g_{dry}, showing no degradation after long-term cycling at higher current. (d) Stable cycling with the leads switched every 200 cycles (at 1 A/g_{dry}), repeatedly reversing the polarity.

4b−d) with a 1 M $PVBr_2$/3 M NaBr electrolyte, paper separator, and symmetric activated carbon electrodes with a 12.7 mg/cm^2 mass loading were assembled and tested by GCD (cell preparation details in the Supporting Information). The two-elecrode cell produced 48.5 $W{\cdot}h/kg_{dry}$ at 0.5 A/g_{dry} (0.44 kW/kg_{dry}) with slow self-discharge (η_R(6 h) = 77%).

Importantly, the PV/Br cell delivers ∼*75% higher* specific energy than the HV/Br cell over a wide range of discharge rates (Figure 4b, from 0.44 kW/kg_{dry} at 0.5 A/g_{dry} to 4.2 kW/kg_{dry} at 10 A/g_{dry}), and maintains stability with 97% energy retention over 10 000 cycles when tested at 2.5 A/g_{dry} (2.0 kW/kg_{dry}) (Figure 4c). For additional characterization, equivalent series resistance (R_{ES}) was measured by both *IR* drop and electrochemical impedance spectroscopy methods (Figure S6 and Table S3).

This system is a hybrid between a supercapacitor and a battery, but unlike batteries, it is not damaged upon polarity reversal. Due to its symmetric nature, fully mixed anolyte/catholyte, and reversible dual solid complexation (i.e., the solids formed at each electrode during charging completely redissolve on discharge), the cell functions identically when operated "backwards" (Figure 4d). The chemistry is therefore tolerant to overdischarge or improper assembly and use, which is important when stacking individual cells into battery packs.[30]

DOI: 10.1021/jacs.6b05038
J. Am. Chem. Soc. 2016, 138, 9373−9376

In conclusion, challenges to maximize the performance of redox ECs are (1) to suppress the diffusion of redox couples in the charged state to prevent side reactions and self-discharge, and (2) to balance the capacity of the electrodes using a catholyte and anolyte that are compatible when intermixed. Our strategy of utilizing *dual redox couples*, each of which participates in a faradaic reaction at one electrode and acts as a complexing agent at the other, solves the main problems associated with redox ECs. With reversible solid complexation of highly soluble PV/Br redox-active electrolytes, the redox EC device retains charged products efficiently, produces a record specific energy with stable cycling, and, unlike other batteries and pseudocapacitors, operates symmetrically. The cells are easy to assemble in air and use simple, inexpensive aqueous redox electrolytes, which suggests they may be manufacturable at low cost and impact applications where performance in-between that of batteries and traditional supercapacitors is desired.

■ ASSOCIATED CONTENT

Supporting Information

The Supporting Information is available free of charge on the ACS Publications website at DOI: 10.1021/jacs.6b05038.

Materials, Figures S1−S7, and experimental details including calculations and cell construction (PDF)

■ AUTHOR INFORMATION

Corresponding Authors

*sjyoo@chem.ucsb.edu
*swb@uoregon.edu
*stucky@chem.ucsb.edu

Author Contributions

#B.E. and S.J.Y. contributed equally.

Notes

The authors declare no competing financial interest.

■ ACKNOWLEDGMENTS

We are grateful to Prof. Martin Moskovits for discussions regarding this work. This work was supported by the Advanced Research Projects Agency-Energy (ARPA-E), U.S. Department of Energy (Award No. DE-AR0000344).

■ REFERENCES

(1) Burke, A. *Electrochim. Acta* **2007**, *53*, 1083.
(2) Zhang, S.; Pan, N. *Adv. Energy Mater.* **2015**, *5*, 1401401.
(3) Yan, J.; Wang, Q.; Wei, T.; Fan, Z. *Adv. Energy Mater.* **2014**, *4*, 1300816.
(4) Ghidiu, M.; Lukatskaya, M. R.; Zhao, M.-Q.; Gogotsi, Y.; Barsoum, M. W. *Nature* **2014**, *516*, 78.
(5) Conway, B. E.; Birss, V.; Wojtowicz, J. *J. Power Sources* **1997**, *66*, 1.
(6) Li, W.; Chen, D.; Li, Z.; Shi, Y.; Wan, Y.; Wang, G.; Jiang, Z.; Zhao, D. *Carbon* **2007**, *45*, 1757.
(7) Kim, S. Y.; Jeong, H. M.; Kwon, J. H.; Ock, I. W.; Suh, W. H.; Stucky, G. D.; Kang, J. K. *Energy Environ. Sci.* **2015**, *8*, 188.
(8) Augustyn, V.; Simon, P.; Dunn, B. *Energy Environ. Sci.* **2014**, *7*, 1597.
(9) Lang, X.; Hirata, A.; Fujita, T.; Chen, M. *Nat. Nanotechnol.* **2011**, *6*, 232.
(10) Rauda, I. E.; Augustyn, V.; Dunn, B.; Tolbert, S. H. *Acc. Chem. Res.* **2013**, *46*, 1113.
(11) Frackowiak, E. In *Supercapacitors: Materials, Systems, and Applications*; Lu, M., Beguin, F., Frackowiak, E., Eds.; Wiley-VCH: Weinheim, 2013; p 207.
(12) Sathyamoorthi, S.; Kanagaraj, M.; Kathiresan, M.; Suryanarayanan, V.; Velayutham, D. *J. Mater. Chem. A* **2016**, *4*, 4562.
(13) Wang, B.; Macia-Agullo, J. A.; Prendiville, D. G.; Zheng, X.; Liu, D.; Zhang, Y.; Boettcher, S. W.; Ji, X.; Stucky, G. D. *J. Electrochem. Soc.* **2014**, *161*, A1090.
(14) Fic, K.; Meller, M.; Frackowiak, E. *Electrochim. Acta* **2014**, *128*, 210.
(15) Frackowiak, E.; Fic, K.; Meller, M.; Lota, G. *ChemSusChem* **2012**, *5*, 1181.
(16) Wang, X.; Chandrabose, R. S.; Chun, S.-E.; Zhang, T.; Evanko, B.; Jian, Z.; Boettcher, S. W.; Stucky, G. D.; Ji, X. *ACS Appl. Mater. Interfaces* **2015**, *7*, 19978.
(17) Frackowiak, E.; Meller, M.; Menzel, J.; Gastol, D.; Fic, K. *Faraday Discuss.* **2014**, *172*, 179.
(18) Chen, L.; Bai, H.; Huang, Z.; Li, L. *Energy Environ. Sci.* **2014**, *7*, 1750.
(19) Akinwolemiwa, B.; Peng, C.; Chen, G. Z. *J. Electrochem. Soc.* **2015**, *162*, A5054.
(20) Chun, S.-E.; Evanko, B.; Wang, X.; Vonlanthen, D.; Ji, X.; Stucky, G. D.; Boettcher, S. W. *Nat. Commun.* **2015**, *6*, 7818.
(21) Bird, C.; Kuhn, A. *Chem. Soc. Rev.* **1981**, *10*, 49.
(22) Monk, P. *The Viologens: Physicochemical Properties, Synthesis and Applications of the Salts of 4,4′-Bipyridine*; John Wiley and Sons Ltd.: Chichester, 1999.
(23) van Dam, H. T.; Ponjeé, J. J. *J. Electrochem. Soc.* **1974**, *121*, 1555.
(24) Zhao, Y.; Ding, Y.; Song, J.; Peng, L.; Goodenough, J. B.; Yu, G. *Energy Environ. Sci.* **2014**, *7*, 1990.
(25) Soloveichik, G. L. *Chem. Rev.* **2015**, *115*, 11533.
(26) Fabjan, C.; Drobits, J. In *Handbook of Battery Materials*, 2nd ed.; Daniel, C., Besenhard, J. O., Eds.; Wiley-VCH: Weinheim, 2011; pp 197−217.
(27) Lancry, E.; Magnes, B.-Z.; Ben-David, I.; Freiberg, M. *ECS Trans.* **2013**, *53*, 107.
(28) Jeon, J. D.; Yang, H. S.; Shim, J.; Kim, H. S.; Yang, J. H. *Electrochim. Acta* **2014**, *127*, 397.
(29) Hoshino, K.; Oikawa, Y.; Sakabe, I.; Komatsu, T. *Electrochim. Acta* **2009**, *55*, 165.
(30) Doughty, D. H. In *Handbook of Battery Materials*, 2nd ed.; Daniel, C., Besenhard, J. O., Eds.; Wiley-VCH: Weinheim, 2011; pp 905−938.

DOI: 10.1021/jacs.6b05038
J. Am. Chem. Soc. 2016, 138, 9373−9376